EAI Endorsed Transactions
on Energy Web

Research Article EAI.EU

Computer Modeling and Parameter Estimation of Power Battery Performance for New Energy Vehicles under Hot Working Conditions

Hua Zhang[1]*

[1]Mechanical and Electrical Engineering Institute, Quzhou College of Technology, Quzhou 324000, China

Abstract

With the aggravation of environmental pollution problems and the reduction of non-renewable energy sources such as oil, new energy vehicles have gradually become the focus of attention, and the application of their power batteries has become more and more widespread. The state of energy (SOE) of the power battery is an important basis for energy scheduling. Therefore, the study used computer technology to develop an analogous model of the power battery and evaluated its properties at various temperatures in order to precisely analyze the performance of the battery under thermal conditions. At the same time, to address the limitations in parameter estimation, the study uses the improved Kalman filter (KF) algorithm to optimize it. The results revealed that the estimation errors of the improved cubature Kalman filter (CKF) algorithm were reduced by 0.52%, 2.91% and 3.10% compared with the traditional CKF algorithm, EKF algorithm and UKF algorithm, respectively. In summary, the research on computer modeling and parameter estimation of the performance of new energy vehicle power batteries under hot working conditions provides important support and reference for the efficient operation and safety of new energy power batteries under hot working conditions.

Keywords: Kalman filter, SOE, New Energy Vehicle, Power Battery, Parameter Estimation

Received on 24 July 2024, accepted on 05 September 2024, published on 06 September 2024

doi: 10.4108/ew.7209

Introduction

Amidst the swift advancements in social and economic spheres, China's vehicle ownership rate keeps rising. Concurrently, the burden of energy consumption and environmental contamination has mounted, and people's awareness of clean energy has progressively expanded. Traditional fuel vehicles need to consume oil, which not only consumes a large amount of non-renewable energy, but also emits exhaust fumes causing serious environmental pollution and greenhouse effect [1]. The primary power battery (PB) for new energy vehicles (NEVs) is now a lithium ion battery (LIB) because of its many benefits, including low self-discharge rate, high energy density, and extended service life [2]. However, LIBs also have some limitations, such as being severely affected by temperature, insufficient range, and unstable operation under complex working conditions [3]. These factors put NEVs at a disadvantage in comparison with traditional fuel vehicles, and many people still prefer to buy fuel vehicles. Therefore, it becomes imperative to improve the performance of PBs for NEVs. The performance of lithium battery (LB) is significantly affected by a variety of uncontrollable factors during the operation of automobiles, especially in high temperature environments and complex working conditions. Thus, to guarantee safe and dependable driving, a precise assessment of the battery's state of energy (SOE) is required. However, current estimation methods are affected by measurement errors, model uncertainty, and system noise, which make it difficult to meet the needs of NEVs. The Kalman filter (KF) algorithm is a recursive filtering technique that has been widely used in the parameter

*Corresponding author. Email: Zzhanghhhua@163.com

estimation (PE) field because it can obtain the optimal estimation of the current state of the dynamic system by utilizing both the observation of the current moment and the state estimation of the previous moment [4]. Therefore, in this context, the study innovatively utilizes computer technology to construct the equivalent model of PB and the improved KF algorithm to enhance the accuracy and efficiency of PE. Therefore, the computer modeling and PE study of the PB performance of NEVs under thermal operating conditions is aimed at obtaining a higher accuracy SOE estimation, which provides a strong support and reference for the safe and reliable operation of NEVs.

1. Literature Review

Since LIBs have a high single operating voltage, small size, low weight, high energy density, and a long cycle life, they are frequently employed in NEV power systems. Many researchers and scholars have conducted in-depth studies on LIBs and achieved a series of results. To maintain the steady and healthy operation of the LIB energy storage system, Zhang M. and other researchers suggested a method of measuring the health state of LIB using impedance spectroscopy. The technique can measure the battery impedance over a broad frequency range, which reflects the battery's aging state. The method's ability to swiftly and reliably evaluate the battery's health status is demonstrated by the results [5]. Xu J et al. proposed a soft-solvent based electrolyte design strategy in order to design an ideal electrolyte with safe characteristics. The strategy balanced between sufficient salt dissociation and desired electrochemical properties under weak Li+-solvent interaction and showed effectiveness with an average Coulombic efficiency of more than 99.9% [6]. To improve the lifetime and safety of high-energy LIBs, Song Y's research team proposed the use of electrode material modification, electrolyte optimization, and diaphragm design to suppress the electrode crosstalk mechanism. The results showed that the method effectively suppressed the crosstalk phenomenon and improved the lifetime and safety of the battery [7]. Huang Z and other researchers suggested replenishing the lost lithium during long-term cycling by adding more active lithium ions to the battery, which would increase the energy density and cycle life of LIBs. The method required no change in the main electrode materials or battery structure and could be compatible with most current LIB production lines, and the results showed the feasibility of the method [8].

KF algorithm works as an important role in PE of PB. To reduce the noise of accelerometer and gyroscope sensors, researchers such as Alfian R I proposed to use the KF algorithm to process the sensor data and optimize the noise attenuation effect. The results showed that the method effectively reduced the noise of the sensor output [9]. To increase the state-of-charge estimate accuracy, Luo Y and other researchers presented a solution that combines the KF algorithm with time-varying battery parameters. The method experimentally obtained battery parameter data at different temperatures, state-of-charge levels, and discharge multiplicities, and utilized these data to update the battery parameters in the matrix of the KF system. According to the findings, the technique successfully raises the state of charge's estimation accuracy [10]. Through the use of aging experimental data from LIBs, Xu W et al. examined the capacity degradation characteristics of batteries in order to improve their efficiency and safety performance. They then identified the equivalent circuit model (ECM)'s online parameters using the adaptive double extended KF algorithm. The outcomes indicated that the maximum error of the battery charge state estimation of this method is only 2.03%, which is effective [11]. To enhance the robustness and accuracy of the indoor positioning system, Feng D and other researchers proposed to use the KF algorithm to build an integrated indoor positioning system by combining ultra-wideband and inertial measurement units. Base stations were reasonably deployed in this system, and the relationship between the accuracy factor and the geometric distribution of base stations was considered. The results demonstrated that the method realized the design of a positioning system with high robustness and continuous tracking capability [12].

In summary, although there are abundant research results for the LIB and KF algorithms, there are relatively few studies on computer modeling and PE for the PB performance of NEVs under hot operating conditions. Therefore, computer modeling and PE for PB performance of NEVs under hot operating conditions are investigated with a view to obtaining higher accuracy of battery SOE estimation.

2. Computer modeling and parameter estimation study of power battery under HWCs

2.1 Equivalent modeling of power battery

There are significant differences in the voltage characteristics of LBs at different temperatures, which directly affect the lifetime and performance of the battery [13]. Therefore, when thinking about extending the lifespan and maximizing performance of LBs, it's critical to examine the SOE performance of the battery under hot working condition (HWC). The chemical processes of the battery's active materials are what drive the charging and discharging of PBs in NEVs, which is basically a transfer between electrochemical and electrical energy [14]. However, the chemical reactions are highly susceptible to temperature fluctuations, which can significantly influence the reaction rate and the generation of side reactions in the battery. This, in turn, affects the performance of the battery [15]. The

chemical reaction principle of LB charging and discharging is shown in Figure 1.

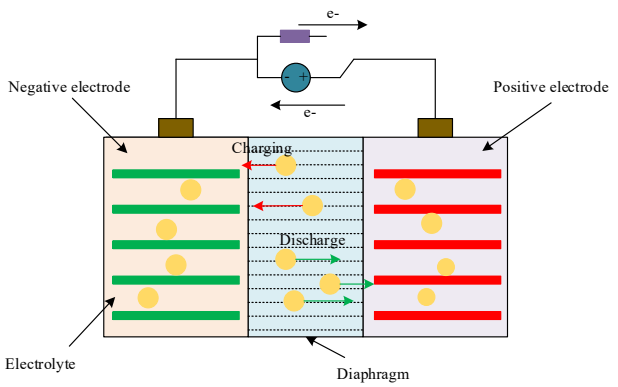

Figure 1. The chemical reaction principle of lithium battery charging and discharging

As shown in Figure 1, chemical reactions such as ohmic polarization, concentration polarization, and electrochemical polarization between the electrolyte and the active material are generated during the charging and discharging process of LB [16]. At low temperatures, the rate of ionic activity in the electrolyte slows down, which can lead to a decrease in the output power of the battery [17]. Furthermore, low temperatures may cause lithium dendrites to grow in the electrolyte, which could short circuit the battery internally and, in extreme situations, even compromise battery safety and life [18].. As the temperature increases, the rate of ionic activity increases and the battery output power increases. However, if the temperature rises above the critical point, the electrolyte releases a significant amount of heat, which renders the active materials less safe. This can result in internal short circuits and battery explosions, which pose a serious risk to the battery's safety. To guarantee the safety of the battery while it is being used, it is vital to take into account how well the battery performs under HWC. To gain insight into the changes of PB under different temperature conditions, it is necessary to use computer technology to construct an equivalent model of the battery for simulation and analysis. Common equivalent models include internal resistance model (IRM), RC model and Thevenin model. Thevenin model can only describe the battery's ohmic polarization, and the RC model can replicate the chemical reaction phenomenon of the battery polarization. The IRM is limited in its ability to precisely simulate battery properties. However, a single set of RC models cannot simulate both polarization phenomena simultaneously. To obtain a more accurate simulation of battery performance, it is therefore examined to incorporate a set of RC circuits based on the classic RC model in combination with the Thevenin model. In Figure 2, the enhanced RC ECM is displayed.

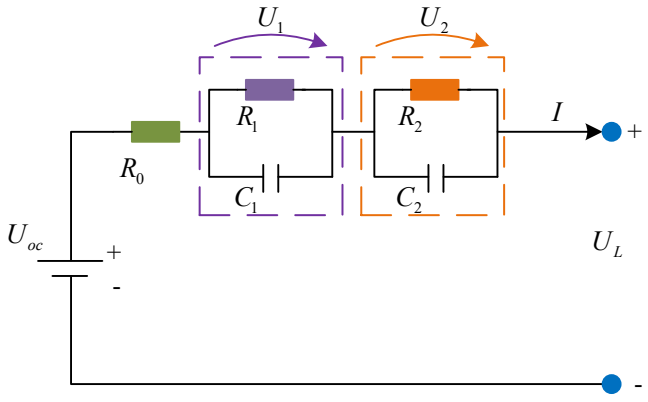

Figure 2. Improved RC ECM

Figure 2 shows the improved RC ECM. R_1 and R_2 are the polarization resistors. U_1 and U_2 are the terminal voltage (TV), and C_1 and C_2 are the polarization capacitance (PC). R_0 denotes the ohmic internal resistance of Thevenin model. U_{oc} and U_L are the open circuit voltage (OCV) and the battery TV, respectively. I is the current. Equation (1) shows the SOE calculation formula for PB.

$$U_{L,k+1} = U_{oc,k+1} + [0,-1,-1]\begin{bmatrix} SOE_k \\ U_{1,k} \\ U_{2,k} \end{bmatrix} - IR_0 + \alpha_k \quad (1)$$

In Equation (1), $U_{L,k+1}$ denotes the cell TV at the moment $k+1$, i.e., the SOE of PB. $U_{oc,k+1}$ denotes the OCV at the moment $k+1$. $U_{1,k}$ and $U_{2,k}$ denote the TV at moment k. SOE_k denotes the cell SOE at the moment k. α_k denotes the measured noise. Since the OCV of the equivalent circuit under HWC varies greatly, it is investigated to characterize the OCV for analytical judgment in order to estimate the battery performance more precisely. The SOE objective function of the OCV under HWC is shown in Equation (2).

$$OCV(SOE) = \sum_{i=1}^{n} \beta_i \times SOE^i + \beta_0 \quad (2)$$

In Equation (2), $OCV(SOE)$ denotes the SOE objective function of the OCV. β_i denotes the coefficients of the i th objective function. n denotes the total number of multiple objective functions, and β_0 denotes the initial coefficients.

2.2 Parameter optimization study based on KF estimation algorithm

The KF algorithm can estimate the state of the system in an optimal way by weighted combination of a priori information and measurements. In battery SOE estimation, the KF algorithm can combine the physical model and the actual measurement data to dynamically update the state estimation and compensate for noise, thereby enhancing the estimation's precision and stability [19]. Thus, the study utilizes the KF algorithm for PE optimization. The cubature Kalman filter (CKF) algorithm in the KF algorithm is a nonlinear filtering method, which solves the problem of poor filtering estimation for high-dimensional systems [20]. The CKF algorithm is suitable for filtering methods for discrete systems. In SOE estimation of PB, the algorithm can utilize the state of the previous moment at each iteration for the estimation of the state of the next moment. Considering the accuracy of the estimated parameters, the study utilizes the CKF algorithm for PE. Figure 3 illustrates the battery performance estimation pipeline with the CKF technique.

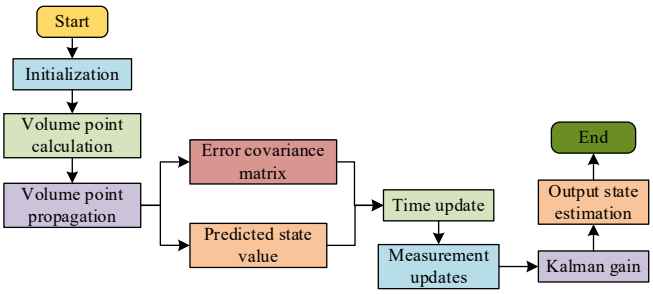

Figure 3. Battery performance estimation process based on CKF algorithm

In Figure 3, in the battery performance estimation process based on the CKF algorithm, the parameter initialization is performed first, and then the volume point calculation in the CKF algorithm is executed and the volume points are propagated. Subsequently, the predicted value of the state is calculated based on the propagated volume points and the error covariance matrix (CM) is calculated. On this basis, a time update is performed, followed by an update based on the measured values. After updating, the Kalman gain is calculated using the state estimates and the updated matrix data. Finally, the state estimates of battery performance are derived from the calculation of Kalman gain. The state variable matrix based on the CKF algorithm is shown in Equation (3).

$$x_{k+1} = Ax_k + BI_k + \varepsilon_k \tag{3}$$

In Equation (3), x_{k+1} denotes the state variable matrix at the $k+1$ moment. A and B denote the state transfer matrix and input matrix, respectively. I_k denotes the current at the moment k and ε_k denotes the process noise. Equation (4) displays the observed variable matrix's expression.

$$y_{k+1} = U_{oc,k+1} + [0,1,1]x_k - IR_0 + \alpha_k \tag{4}$$

In Equation (4), y_{k+1} denotes the matrix of observed variables at the $k+1$ moment. The observed variable matrix and the state variable matrix show how closely the current state and the battery performance estimation based on the CKF method are related. But sudden changes in the current cause the algorithm to track poorly, which compromises the precision and effectiveness of the SOE estimation of the PB. To address this limitation, the study improves the CKF algorithm by utilizing fuzzy theory on its basis. By combining the CKF algorithm with fuzzy theory to construct a fuzzy controller, the dynamic adjustment of Kalman gain can be realized. The introduction of the fuzzy factor enables the system to respond to sudden current changes more flexibly, thus improving the efficiency and accuracy of the PE. Equation (5) displays the CM of the enhanced CKF method based on the fuzzy factor.

$$P_{k|k-1} = \frac{1}{2n}\sum_{i=1}^{2n}\left(G_{i,k|k-1}G^{T}_{i,k|k-1} - \hat{g}_{i,k|k-1}\hat{g}^{T}_{i,k|k-1}\right) + \lambda\xi \tag{5}.$$

In Equation (5), $P_{k|k-1}$ denotes the CM based on k moments and $k-1$ moments. T denotes the matrix transpose. $\hat{g}$ and G denote the simulated and observed values of the end voltage, respectively. λ and ξ denote the output and observation noise variance of the fuzzy controller, respectively. Figure 4 displays the SOE estimation framework diagram based on the upgraded CKF method.

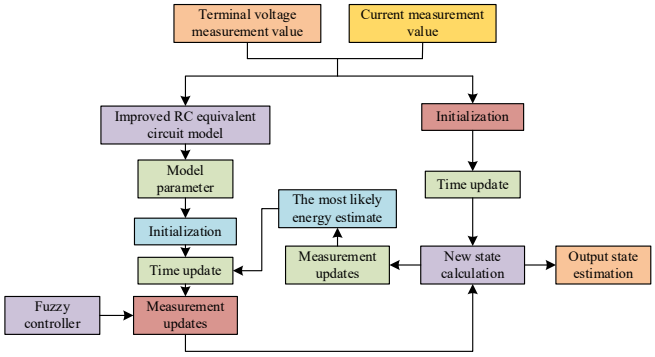

Figure 4. SOE estimation framework diagram based on improved CKF algorithm

The SOE estimation framework, which utilizes the improved CKF algorithm (ICKFA), first initializes parameters such PC and polarization resistance in the created enhanced RC ECM, as shown in Figure 4. Then, time updating and measurement updating are performed and combined with a fuzzy controller to obtain the estimated value of SOE. Subsequently, an updated computation is carried out using the current and TV observed values to generate the most likely energy estimate. This estimated value is used for the next iteration and is input to the time update process of the SOE estimate to perform the correction of the SOE estimate. Through such a process, the value obtained is the result of the correction of the two states, which allows to improve the estimation accuracy.

3. Result

3.1 Experimental environment setup

The investigation carried out an experimental environment established for HWC in order to validate the effectiveness of SOE estimation based on the ICKFA. To monitor the battery temperature, the study placed four temperature sensors on each of the four sides of the LB to collect temperature data. These four sensors are labeled as temperature measurement points (TMP) 1 to 4 and are located at the front, side, bottom and center of the battery, respectively. To simulate HWC, the study creates different temperature environments using a Model LW-150 high and low temperature tester. The battery test system is model NBT5V100AC8-T, and the collected data information is sent to a computer via a communication module for display and storage. The computer system used is Ubuntu 16.04.7 LTS, with 32GB of RAM and Intel Core i7-9700 processor. The used LB has a voltage setting range of 0-5V and a current setting range of 300mA-100A. Its rating is 17Ah. Table 1 displays the precise setup of the experimental setup.

Table 1. Specific experimental environment configuration

Experimental equipment	Model/Configuration
Temperature sensors	Mark temperature measurement points 1 to 4 respectively, located on the front, side, bottom, and center of the battery
Test chamber	LW-150 high-low temperature test chamber
Battery test system	Model NBT5V100AC8-T
Computer system	Ubuntu 16.04.7 LTS, 32GB RAM, Intel Core i7-9700 Processor
Lithium battery	Rated capacity 17Ah, voltage range 0V to 5V, current range 300mA to 100A

3.2 Estimated performance analysis of power battery under HWC

To validate the estimation performance of PB under HWC, the study utilizes the SOE estimation model based on the ICKFA to estimate the voltage during charging and discharging of batteries at different temperatures. Figure 5 displays the variation curves of the electric capacity versus the voltage at different temperatures. In Figure 5(a), the voltage decreases gradually with the increase of temperature during the battery charging process. At the beginning of charging, the maximum voltage at -20°C is 4.2 V, while the minimum voltage at 40°C is 3.5 V. In Figure 5(b), contrary to the charging process, the higher the temperature, the higher the voltage in the discharging process. Comprehensively, it can be concluded that the SOE estimation model based on the ICKFA accurately estimates the voltage changes in the battery charging and discharging process, which indicates that it is able to efficiently perform PB performance estimation under HWC.

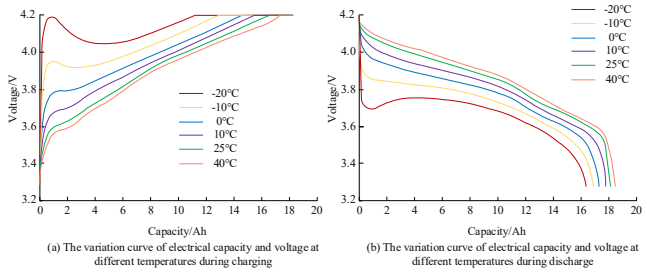

Figure 5. The capacitance and voltage fluctuation curves at various temperatures

To further verify the performance of the estimation model, this study sets 1C multiplicity 2C multiplicity and 3C multiplicity discharge multiplicity for experimental analysis, respectively. The estimation accuracy of each TMP under different discharge multiples is shown in Table 2. The SOE estimation model, which has a strong estimation performance, has estimation accuracy of more than 96% at various discharge multiples based on the ICKFA. The TMP 3 is the most accurate, with an estimation accuracy of greater than 99%. This is because the point is positioned in the middle of the battery, meaning that the temperature it collects is more likely to represent the battery's actual temperature. This further confirms that the method has high estimation accuracy.

Table 2. Estimated accuracy of temperature measurement points at different discharge rates

Discharge rate		Temperature measurement points			
		No.1	No.2	No.3	No.4
1C	Estimated value/℃	32.08	32.23	32.26	32.05
	Actual value/℃	31.75	31.81	31.96	31.16
	Estimation accuracy/%	98.97	98.69	99.07	97.22
2C	Estimated value/℃	38.77	39.02	39.05	38.72
	Actual value/℃	38.59	38.76	39.10	37.63
	Estimation accuracy/%	99.53	99.33	99.87	97.18
3C	Estimated value/℃	45.17	45.53	45.59	45.15
	Actual value/℃	44.70	45.12	45.63	43.74
	Estimation accuracy/%	98.95	99.09	99.91	96.87

3.3 Performance validation of SOE estimation for power battery

The study is conducted to conduct discharge tests at 25°C room temperature state and 40°C HWC, respectively, with a discharge multiplier of 1C, in order to validate the performance of SOE estimation based on the ICKFA. The simulated wave-forms of SOE estimation based on the ICKFA were plotted as shown in Figure 6. In Figure 6(a), the SOE of the PB shows a linear decrease with the increase of time at 25°C room temperature, which is consistent with the actual SOE change rule. In addition, the estimated and theoretical values show a high degree of overlap with each other, and their waveform curves are all within the boundary range. In Figure 6(b), the simulated waveform of SOE estimation still fluctuates within the boundary range at 40°C HWC. It shows that the SOE estimation performance based on the ICKFA has high robustness and good estimation effect.

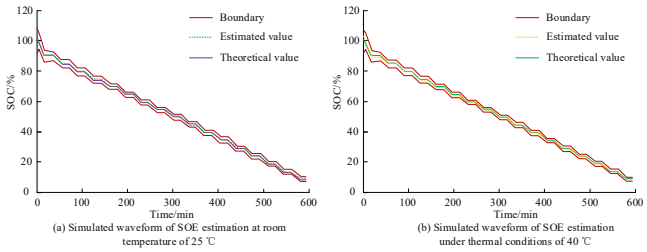

Figure 6. SOE estimation simulation waveform based on improved CKF algorithm

To further validate the performance effect of SOE estimation based on the ICKFA, the study statistically analyzed the estimation error (EE) of SOC at different temperatures, as shown in Table 3. At -20°C temperature, the maximum EE reaches 3.56% when SOC≤30%. While at 10°C temperature, the lowest EE is only 0.26% for 30%<SOC<80%. This indicates that the lower the temperature, the higher the EE, whereas at other temperatures, there is no significant change in the EE. The greatest EE of 0.82% for SOC ≥ 80% is seen at a high temperature of 40°C, suggesting that the SOE estimate utilizing the ICKFA still maintains a good estimation accuracy under HWC.

Table 3. Estimation error of SOC at different temperatures

Temperature/ ℃	Estimation error/%		
	SOC≤30 %	30%<SOC<80 %	SOC≥80 %
-20	3.56	1.06	2.12
-10	3.06	1.03	2.06
0	1.92	0.92	1.87
10	0.77	0.26	0.64
25	0.76	0.34	0.71
40	0.79	0.46	0.82

To validate the superior performance of SOE estimation based on the ICKFA, the study validates the method in comparison with other estimation algorithms. The other estimation algorithms include the traditional CKF algorithm, extended Kalman filter (EKF) algorithm and unscented Kalman filter (UKF) algorithm. Figure 7 displays the error variation curves for various estimate strategies. With the lowest EE curve and a rapid convergence state, the ICKFA is the most accurate and efficient estimator. While the greatest errors of the conventional CKF method, the EKF algorithm, and the UKF algorithm are 1.58%, 3.97%, and 4.16%, respectively, the maximum error of the ICKFA is 1.06%. The mistakes based on the ICKFA are decreased by 0.52%, 2.91%, and 3.10%, in comparison to these algorithms. To summarize, the utilization of the ICKFA in SOE estimate results in enhanced efficiency and accuracy of estimation.

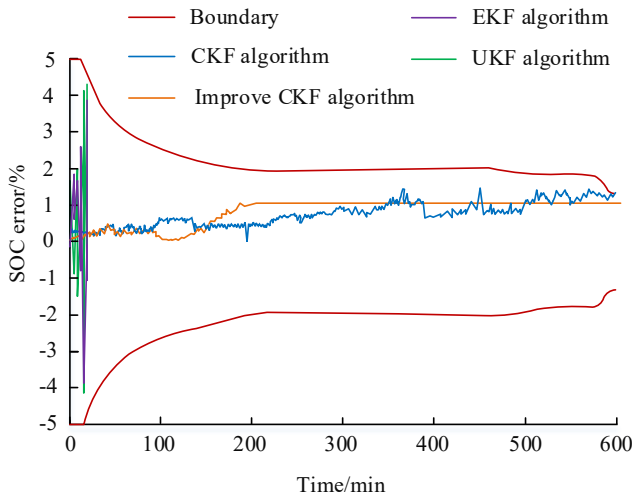

Figure 7. Error variation curves of different estimation algorithms

4. Conclusions

Due to the rapid development of NEV in recent years, there has been an emphasis on the investigation of PB performance. The study employs the revised KF algorithm to assess the state of PB and examines its performance under HWC. The outcomes revealed that the estimation accuracy of the SOE estimation model based on the ICKFA exceeded 96% at different discharge multiplicities, with the highest estimation accuracy at the TMP No. 3, which all exceeded 99%. This indicated that the ICKFA has high accuracy and reliability for the estimation of PB states. Under the high temperature condition of 40°C, the maximum EE was 0.82% at SOC ≥ 80%, which indicates that the SOE estimation based on the ICKFA can still maintain a high accuracy under different HWC. The ICKFA reduced its EE by 0.52%, 2.91% and 3.10% compared with the traditional CKF algorithm, EKF algorithm and UKF algorithm, respectively. This indicated that the ICKFA effectively improved the SOE estimation accuracy and efficiency. In summary, the study of computer modeling and PE of the PB performance of NEVs under HWC achieved high accuracy and efficiency of battery performance estimation, which provides support and reference for the study of the PB performance of NEVs. However, the study only discusses the battery performance estimation under HWC and does not investigate the performance at extreme temperatures, so the results are not comprehensive enough, and this aspect needs to be further improved.

Acknowledgements

This research was supported by Project of Zhejiang Provincial educational science planning（2019SCG130）and Project of Zhejiang Provincial Higher Education Institute（KT2022288.

References

[1] A. Beaucamp, M. Muddasar, I. S. Amiinu, M. M. Leite, M. Culebras, K. Latha, and M. N. Collins, "Lignin for energy applications–state of the art, life cycle, technoeconomic analysis and future trends," Green Chemistry, vol. 24, no. 21, pp. 8193-8226, 2022. doi: 10.1039/D2GC02724K.

[2] K. Szulecki and I. Overland, "Russian nuclear energy diplomacy and its implications for energy security in the context of the war in Ukraine," Nature Energy, vol. 8, no. 4, pp. 413-421, 2023. doi: 10.1038/s41560-023-01228-5.

[3] J. Xu, X. Cai, S. Cai, Y. Shao, C. Hu, S. Lu, and S. Ding, "High-energy lithium-ion batteries: recent progress and a promising future in applications," Energy & Environmental Materials, vol. 6, no. 5, pp. 12450-12459, 2023. doi: 10.1002/eem2.12450.

[4] C. D. Quilty, D. Wu, W. Li, D. C. Bock, L. Wang, L. M. Housel, and E. S. Takeuchi, "Electron and ion transport in lithium and lithium-ion battery negative and positive composite electrodes," Chemical Reviews, vol. 123, no. 4, pp. 1327-1363, 2023. doi: 10.1021/acs.chemrev.2c00214.

[5] M. Zhang, Y. Liu, D. Li, X. Cui, L. Wang, L. Li, and K. Wang, "Electrochemical impedance spectroscopy: A new chapter in the fast and accurate estimation of the state of

health for lithium-ion batteries," Energies, vol. 16, no. 4, pp. 1599-1606, 2023. doi: 10.3390/en16041599.

[6] J. Xu, J. Zhang, T. P. Pollard, Q. Li, S. Tan, S. Hou, and C. Wang, "Electrolyte design for Li-ion batteries under extreme operating conditions," Nature, vol. 614, no. 7949, pp. 694-700, 2023. doi: 10.1038/s41586-022-05627-8.

[7] Y. Song, L. Wang, L. Sheng, D. Ren, H. Liang, Y. Li, and X. He, "The significance of mitigating crosstalk in lithium-ion batteries: a review," Energy & Environmental Science, vol. 16, no. 5, pp. 1943-1963, 2023. doi: 10.1039/D3EE00441D.

[8] Z. Huang, Z. Deng, Y. Zhong, M. Xu, S. Li, X. Liu, and Y. Huang, "Progress and challenges of prelithiation technology for lithium-ion battery," Carbon Energy, vol. 4, no. 6, pp. 1107-1132, 2022. doi: 10.1002/cey2.256.

[9] R. I. Alfian, A. Ma'arif, and S. Sunardi, "Noise reduction in the accelerometer and gyroscope sensor with the Kalman filter algorithm," Journal of Robotics and Control (JRC), vol. 2, no. 3, pp. 180-189, 2021. doi: 10.18196/jrc.2375.

[10] Y. Luo, P. Qi, Y. Kan, J. Huang, H. Huang, J. Luo, and S. Zhao, "State of charge estimation method based on the extended Kalman filter algorithm with consideration of time-varying battery parameters," International Journal of Energy Research, vol. 44, no. 13, pp. 10538-10550, 2020. doi: 10.1002/er.5687.

[11] W. Xu, S. Wang, C. Jiang, C. Fernandez, C. Yu, Y. Fan, and W. Cao, "A novel adaptive dual extended Kalman filtering algorithm for the Li-ion battery state of charge and state of health co-estimation," International Journal of Energy Research, vol. 45, no. 10, pp. 14592-14602, 2021. doi: 10.1002/er.6719.

[12] D. Feng, C. Wang, C. He, Y. Zhuang, and X. G. **a, "Kalman-filter-based integration of IMU and UWB for high-accuracy indoor positioning and navigation," IEEE Internet of Things Journal, vol. 7, no. 4, pp. 3133-3146, 2020. doi: 10.1109/JIOT.2020.2965115.

[13] J. Lv, B. Jiang, and X. Wang, "Estimation of the state of charge of lithium batteries based on adaptive unscented Kalman filter algorithm," Electronics, vol. 9, no. 9, pp. 1425-1431, 2020. doi: 10.3390/electronics9091425.

[14] H. Li, H. Qi, H. Cao, and L. Yuan, "Industrial policy and technological innovation of new energy vehicle industry in China," Energies, vol. 15, no. 24, pp. 9264-9269, 2022. doi: 10.3390/en15249264.

[15] I. S. Sorlei, N. Bizon, P. Thounthong, M. Varlam, E. Carcadea, M. Culcer, and M. Raceanu, "Fuel cell electric vehicles—A brief review of current topologies and energy management strategies," Energies, vol. 14, no. 1, pp. 252-258, 2021. doi: 10.3390/en14010252.

[16] A. König, L. Nicoletti, D. Schröder, S. Wolff, A. Waclaw, and M. Lienkamp, "An overview of parameter and cost for battery electric vehicles," World Electric Vehicle Journal, vol. 12, no. 1, pp. 21-26, 2021. doi: 10.3390/wevj12010021.

[17] Y. Zhu, X. Li, Q. Liu, S. Li, and Y. Xu, "A comprehensive review of energy management strategies for hybrid electric vehicles," Mechanical Sciences, vol. 13, no. 1, pp. 147-188, 2022. doi: 10.5194/ms-13-147-2022.

[18] H. Farhadi Gharibeh and M. Farrokhifar, "Online multi-level energy management strategy based on rule-based and optimization-based approaches for fuel cell hybrid electric vehicles," Applied Sciences, vol. 11, no. 9, pp. 3849-3856, 2021. doi: 10.3390/app11093849.

[19] T. Deng, P. Tang, Z. Su, and Y. Luo, "Systematic design and optimization method of multimode hybrid electric vehicles based on equivalent tree graph," IEEE Transactions on Power Electronics, vol. 35, no. 12, pp. 13465-13474, 2020. doi: 10.1109/TPEL.2020.2990209.

[20] G. G. Farivar, W. Manalastas, H. D. Tafti, S. Ceballos, A. Sanchez-Ruiz, E. C. Lovell, and J. Pou, "Grid-connected energy storage systems: State-of-the-art and emerging technologies," Proceedings of the IEEE, vol. 111, no. 4, pp. 397-420, 2022. doi: 10.1109/JPROC.2022.3183289.